Acta Cryst. (1995). D**51**, 354–367

Refined Crystal Structure of Lysozyme from the Rainbow Trout (*Oncorhynchus mykiss*)

BY SOLVEIG KARLSEN, BJØRN E. ELIASSEN, LARS KR. HANSEN, ROLF L. LARSEN, BJØRN W. RIISE, ARNE O. SMALÅS AND EDWARD HOUGH*

Department of Chemistry, Institute of Mathematical and Physical Science, University of Tromsø, N-9037 Tromsø, Norway

AND BJØRN GRINDE

National Institute of Public Health, Geitmyrsveien 75, 0462 Oslo 4, Norway

(*Received* 15 *April* 1994; *accepted* 22 *September* 1994)

Abstract

Lysozymes (E.C. 3.2.1.17) are well characterized ubiquitous enzymes that have an antibacterial effect. The lysozymes from rainbow trout (RBTL) (*Oncorhynchus mykiss*) could be particularly interesting in aquaculture since they show higher activity than egg-white lysozyme and lysozymes from other fish species against a variety of pathogenic bacteria. Two lysozymes, I and II, differing only in a single amino acid, were purified from the kidney of rainbow trout and shown to belong to the *c*-type class of lysozymes. The type II form was shown to be much more potent against a variety of bacteria than the type I enzyme. We have grown crystals from a mixture containing about 80% type I and 20% type II lysozyme from rainbow trout, and solved the X-ray crystal structure. The crystals are trigonal with $a = 76.68$, $c = 54.46$ Å and space group $P3_121$. The phase problem was solved by the molecular-replacement method, and the structure was refined to an *R* factor of 17.4% using data to 1.8 Å resolution. The crystal structure shows that the three-dimensional structure of rainbow trout lysozyme is very similar to the previously solved structures of other *c*-type lysozymes. The single polypeptide of 129 amino acids is folded into two domains separated by a deep cleft which contains the active site. Secondary-structure elements, four α-helices and a three-stranded β-sheet, are located in the same sequential positions as in the hen, turkey and human enzymes. The β-sheet is found to be common for structures of both *c*- and *g*-type lysozymes. We suggest that differences in antibiotic activity of the two forms of RBTL are probably due to small differences in the hydophobicity of a small surface region.

Introduction

Lysozymes destroy bacteria by attacking their cell walls. The typical *c*-type lysozymes, including the rainbow trout enzyme, are 1,4-β-acetyl-muramidases, *i.e.*, they selectively cleave the glycosidic bond between the C1 atom of *N*-acetylmuramic acid (NAM) and the O4 atom of *N*-acetylglucosamine (NAG) (Salton & Ghuysen, 1959, 1960) in the peptidoglycan of bacterial cell walls.

Lysozymes form part of the non-specific immune defence system in most animals. They are particularly important in the bacterial defence of invertebrates and lower vertebrates since these organisms have a less elaborate specific immune defence than higher vertebrates. The ability of lysozymes to lyse bacteria has made them commercially interesting, both as purified proteins, and as target enzymes in transgenic strategies directed towards improving the immune defence of species, such as salmon, which are used in aquaculture.

In screening for lysozyme activity in various fish species, the rainbow trout (*Oncorhynchus mykiss*, formerly *Salmo gairdneri*) was found to contain a much higher level of activity than any other species (Grinde, Lie, Poppe & Salte, 1988). Two lysozymes were found in this fish, differing only in a single amino acid. Type I has Asp in position 86 while type II has an Ala in this position, giving them slightly different isoelectric points (Grinde, Jolles & Jolles, 1988; Dautigny *et al.*, 1991). The 129 amino acids of the mature rainbow trout lysozyme share 78 amino acids with the chicken enzyme and 88 amino acids with the human form. These enzymes are clearly evolutionary conserved and have closely related biochemical properties. However, when tested for their ability to disrupt or inhibit growth of bacteria, obvious differences were observed (Grinde *et al.*, 1988; Grinde, 1989*a*,*b*). Both types of rainbow trout lysozyme had a higher specific activity in *Micrococcus luteus* lysis assay than hen-egg-white lysozyme, the type II enzyme more than three times as high. Furthermore, the type II enzyme in particular has been shown to be much more potent against a variety of pathogenic bacteria, both Gram positive and Gram negative. This includes bacteria which cause serious problems in salmon aquaculture.

Enzyme-kinetics studies have shown that the rainbow trout lysozymes have higher catalytic activity below

* Author to whom correspondence should be addressed.

ISSN 0907-4449

293 K than the hen enzyme. This is appropriate to cold-adapted fish species (Grinde *et al.*, 1988).

Medical interest in lysozymes is not restricted to their antibacterial potential. It has recently been shown that either of two mutations in the gene for human lysozyme is the cause of an hereditary form of amyloidosis (Pepys *et al.*, 1993). This disease is autosomal dominant and usually fatal by the fifth decade. The mutation involves exchange of threonine for isoleucine at position 56 and histidine for aspartic acid at residue 67, residues which are highly conserved between human, rainbow trout and other *c*-type lysozymes (Jolles & Jolles, 1984). Structural information on the rainbow trout enzyme may help elucidate why the mutated forms cause the formation of amyloid fibrils and to assist on the engineering of novel lysozymes with properties tailored for specific purposes.

In the present paper we describe the crystal structure of rainbow trout lysozyme (RBTL), and compare it with the previously solved structure of lysozyme from hen egg-white (HEWL), turkey egg-white (TEWL), human (HUML) and Australian black swan egg-white (SELg).

Experimental

Crystallization

The two rainbow trout lysozymes, designated I and II, were purified as described previously (Grinde *et al.*, 1988).

Crystals suitable for X-ray structure studies were obtained after extensive screening. A preliminary pH/$(NH_4)_2SO_4$ screening, using the hanging-drop vapour-diffusion method, was carried out at 277 K using ACP buffer (0.1 *M* acetate, 0.1 *M* citrate, 0.1 *M* phosphate) at varying pH values. These experiments were carried out using a mixture of about 80% of type I and 20% of type II lysozyme (18 mg ml^{-1}) and 30–45% saturated solutions of ammonium sulfate at pH 4 to 10. Needle-shaped crystals appeared after 2 weeks in the pH range 5–10 at 30–45% saturated $(NH_4)_2SO_4$.

Further hanging-drop experiments were then carried out at 277 K and room temperature and with glycine–NaOH buffer (0.5 *M* in the reservoir) and 25–32.5% saturated solutions of ammonium sulfate over the pH range 8.5–11.0. Well defined crystals appeared at pH 9.0 to 11.0 and 27.5 to 32.5% saturation of $(NH_4)_2SO_4$. Crystals, up to 0.8 mm, grew at 277 K, while smaller crystals appeared at room temperature.

Since crystals were obtained from a mixture containing both types of the enzyme, they had to consist of either type I, type II or a mixture of both types. Separately, crystallization experiments with pure type I or II showed that both types gave crystals with the same appearance and cell dimensions, provided crystallization conditions were the same. This implies that the three-dimensional structures of the lysozymes and the packing of the molecules must be very similar which is not surprising taking into consideration that the two lysozymes differ only in a single amino acid (Dautigny *et al.*, 1991). Unfortunately, specimens of the separated forms were available in insufficient amounts for data collection.

Table 1. *Summary of results and conditions for the data collection*

Space group	$P3_121$
Cell parameters (Å, °)	$a = b = 76.68$, $c = 54.46$ $\alpha = \beta = 90.0$, $\gamma = 120.0$
Mosaicity (°)	0.31
Resolution (Å)	42.11–1.80
Completeness (%)	91.20
No. of independent reflections ($F > 1\sigma_F$)	16305
Overall R_{merge} (%)*	4.17

* $R_{merge} = \sum |I_i - \langle I \rangle| / \sum I_i$, where I_i is the intensity of an individual reflection and $\langle I \rangle$ is the mean intensity of that reflection.

Data collection

Preliminary X-ray studies on rainbow trout lysozyme using the precession technique showed that the crystals diffract to at least 1.8 Å. An Enraf–Nonius CAD-4 diffractometer was used to determine the unit-cell dimensions and space group. The space group was found to be $P3_121/P3_221$ with preliminary cell dimensions $a = b = 76.9$ and $c = 54.6$ Å for both types.

Data sets were collected on a Siemens Xentronics area detector system in Madison, Wisconsin and a Rigaku Automated X-ray Imaging Systems (R-AXIS II) at Molecular Structure Corporation (MSC) in Houston, Texas, using crystals grown from the mixed batch. Due to the higher resolution (1.80 and 1.92 Å, respectively) and higher degree of completeness (91.2 and 80%, respectively) of the image-plate data in comparison to the Siemens MWPC data set, the latter data were not used in the structure determination.

A summary of results and conditions for the data collection on the R-AXIS II is given in Table 1. A total of 70573 accepted observations ($|F| > 1\sigma_F$) were measured. These were reduced to a unique set of 16305 reflections to 1.80 Å resolution. R_{merge} for equivalent reflections measured on 60 frames was 4.17%.

Structure solution

Structure solution was carried out using the integrated package of molecular-replacement programs *MERLOT*, Version 2.3 (Fitzgerald, 1988).

Due to similar molecular weight and N-terminal sequences (Grinde *et al.*, 1988), the most studied example of the *c*-type lysozymes, hen egg-white lysozyme, was selected as the most suitable search object for molecular replacement. The complete primary structure of the rainbow trout lysozymes, which became available later (Dautigny *et al.*, 1991), shows that human

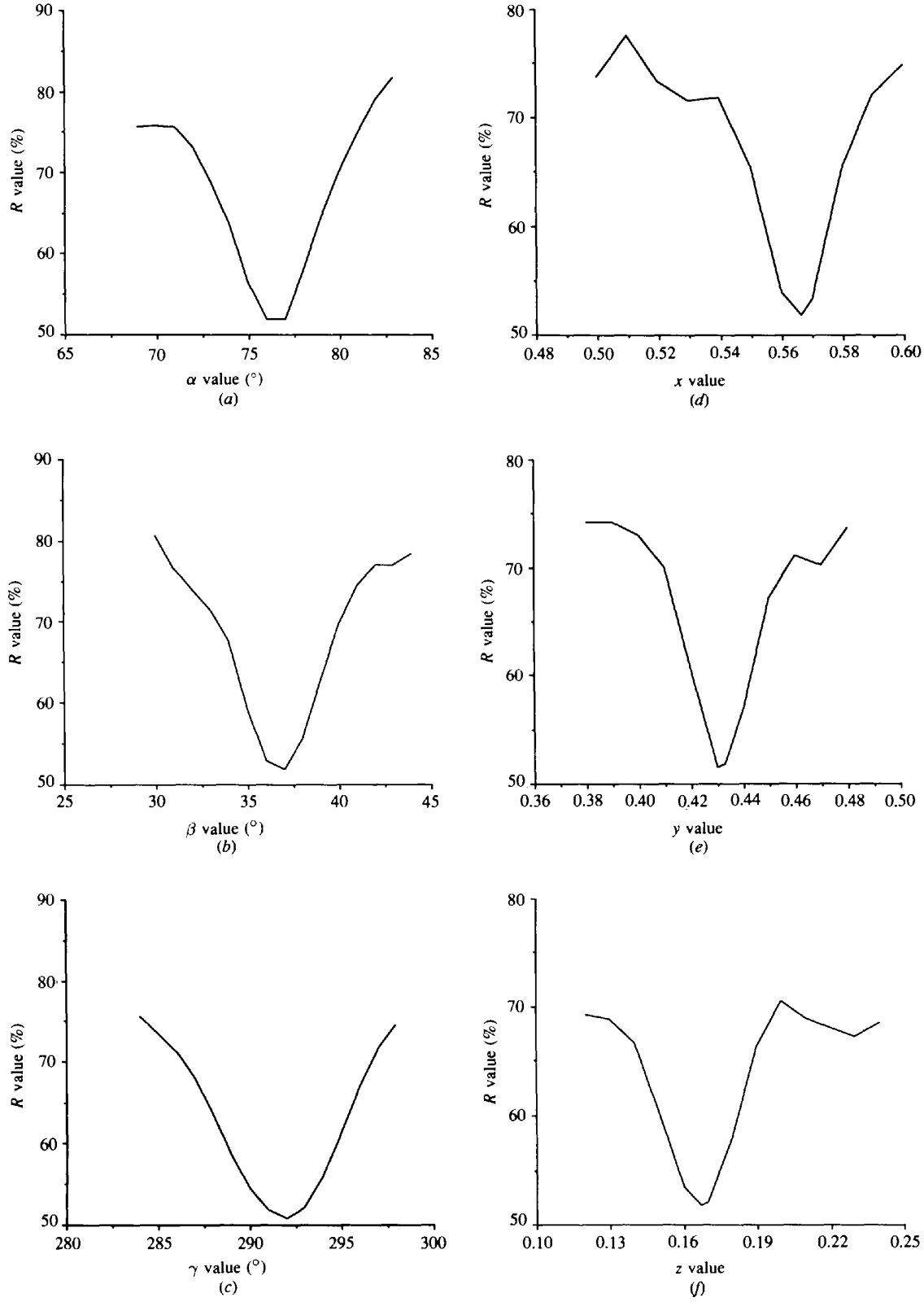

Fig. 1. Effect on R factor of rotation in (*a*) α, (*b*) β and (*c*) γ and translations in (*d*) x, (*e*) y and (*f*) z around the correct solutions. For each rotation or translation the five other parameters were kept constant.

lysozyme would possibly have been a better model due to greater sequence homology. The refined structure of hen egg-white lysozyme (Hodson, Brown, Sieker & Jensen, 1990) from the Protein Data Bank (entry 1LTZ) at Brookhaven National Laboratory was used as search model. This has been refined to an R value of 0.254, on data to 1.97 Å. The complete structure with all side chains but omitting water, was used in the rotation searches.

Before the rotation searches were carried out, structure factors for the HEWL model were computed in an artificial triclinic cell with orthogonal axes of length 130 Å. The model was given an overall temperature factor of 15 Å^2.

Initial searches with the Crowther fast-rotation function (Crowther, 1972) were carried out varying the upper resolution limit from 3.5 to 6.0 Å and the lower resolution limit from 10.0 to 13.0 Å. Since the number of F_{calc}'s used in the rotation function was program limited, weak structure factors were omitted, and threshold values at each resolution range were chosen so that a maximum could be used. Furthermore, only $F_{obs} > 2\sigma_F$ were included in the calculations. In order to reduce the effect of intermolecular vectors, a Patterson cut-off radius was used in the rotation searches for each resolution range. The rotation searches were carried out over the unique Patterson space using the three Eulerian angles α, β and γ (α, 0–120° in steps of 1.67°; β, 0–90° in steps of 3.0°; γ, 0–360° in steps of 5.0°).

For the Lattman rotation searches (Lattman, Nockolds, Kretsinger & Love, 1971) and the Crowther & Blow (1967) translation searches, data from different resolution ranges from 4.0 to 13.0 Å were used, and a continuous transform was formed from the calculated structure factors for the HEWL model. Lattman rotation-function searches were carried out in steps of 3° in α, β and γ. Crowther & Blow translation-function searches were carried out for the HEWL model in fractional steps of 0.02 in all three axial directions, and over eight different resolution ranges from 4.1 to 13.0 Å.

For the Crowther rotation searches, the best-resolved peaks appeared at a maximum resolution from 4.0 to 4.5 Å and a minimum resolution of 11.0–13.0 Å. The rotation searches indicated that the solution could be from 73 to 80° in α, from 36 to 40° in β and from 290 to 300° in γ. The Lattman rotation-function search, which usually yields more precise rotation angles, gave a peak at $\alpha = 76°$, $\beta = 36°$ and $\gamma = 291°$. These rotation angles were applied to the HEWL model, and Crowther & Blow translation searches were carried out for different resolution ranges for both enantiomorphs ($P3_121$ and $P3_221$). However, a consistent set of translation vectors was only found for $P3_121$ and for this space group Harker peaks at $x = 0.57$, $y = 0.43$ and $z = 0.17$ were observed in all the Patterson maps.

R-factor minimization of these rotation and translation parameters, using the program *RMINIM* in *MERLOT*, gave an R factor of 0.504 for data between 4.1 and 12.0 Å. The R value dropped by 25% when the correct rotation and translation solutions were reached. This is illustrated in Fig. 1. The refined parameters were similar to the original solution, $\alpha = 76.20°$, $\beta = 36.70°$, $\gamma = 291.30°$, $x = 0.57$, $y = 0.43$ and $z = 0.16$. 107 unique intermolecular contacts shorter than 3 Å were found by the program *CONTACT* between the HEWL model and its neighbouring molecules. The majority of these contacts involve side chains where a short side chain in RBTL has been replaced by a much larger one in HEWL, *e.g.* Ala21 and Gly128 in RBTL is replaced by two arginines in HEWL. In the refined structure of the rainbow trout lysozyme, a short hydrogen bond (2.5 Å) is seen between the main-chain CO group of Gly128 and the main-chain NH group of Ala21 in a neighbouring molecule.

Molecular-replacement studies with a HEWL model where amino acids in the primary structure of the HEWL model were replaced by those in RBTL, were also carried out. Before molecular replacement, energy minimalization and molecular dynamics were carried out using the

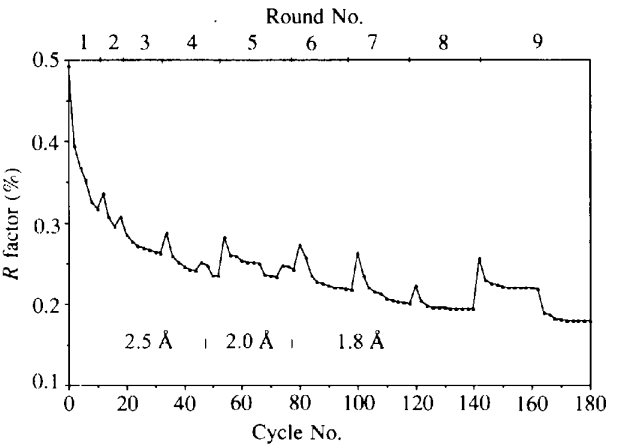

Fig. 2. Progress of the refinement of the rainbow trout lysozyme structure. R factor as function of refinement cycle. The refinement rounds are marked on the top of the plot frame, and the resolution of data used in the refinement is included in the plot.

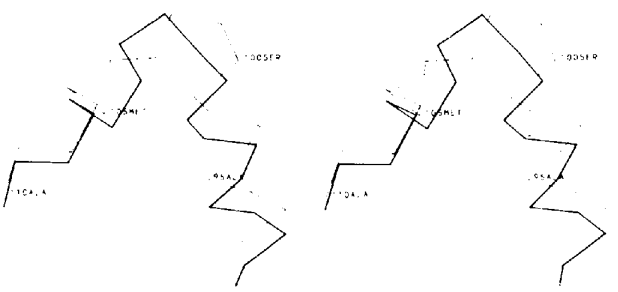

Fig. 3. C_α skeletons from residues 90 to 110 showing the different folding of the loop region from residues 99 to 106 in RBTL (thick lines) and HEWL (thin lines). Residues are labelled according to the amino-acid sequence of HEWL.

program *CHARMm* to minimize local strain (Brooks *et al.*, 1983). The rotation and translation solutions using this model were not significantly different to those obtained with the original HEWL model.

Refinement

Refinement of the structure of the rainbow trout lysozyme was carried out by restrained least squares using *PROLSQ* with standard geometric restraints (Hendrickson, 1985) from the *CCP*4 package (Collaborative Computational Project, Number 4, 1994). Model building was carried out using the program *FRODO* (Jones, 1985) on an Evans & Sutherland PS300 colour graphics system. Refinement and map calculations were run on a Vax 8600 computer.

The initial R factor for HEWL oriented and positioned according to the molecular-replacement solution, was 50.4% for data from 8.0 to 2.5 Å resolution, In order to get a more correct starting structure for the model, amino acids were substituted to give the primary sequence of the rainbow trout lysozyme.

The resulting RBTL model was refined without prior rigid-body refinement. After 11 cycles of refinement, the model converged with an R factor of 31%. After three rounds of refinement and model building the resolution was extended to 2.2 Å for four rounds of refinement and then the full data set (1.8 Å) was included in the calculations. Refinements from rounds three to ten were completed with 2–4 cycles of individual B-factor refinement with atomic coordinates kept constant.

Electron-density maps for model building were calculated with $2F_o - F_c$ and $F_o - F_c$ coefficients. The model and the electron-density maps were studied after each refinement run. Omit maps were calculated after 11 cycles of *PROLSQ* refinement for uncertain regions. In regions of the structure where we found differences between model and electron density and where temperature factors indicated that atoms should be moved, manual adjustments of the model were made using *FRODO*.

Refinement after initial model building, which mainly comprised fitting the main chain and side chains in easily interpretable areas, and deletion of side chains that were misplaced, lowered the R factor to 29% for data from 8.0 to 2.5 Å. The next two model-building and refinement rounds lowered the R value to 24%, with data to 2.2 Å resolution. From round 5 data to 1.8 Å were included, and the R factor dropped to 17% after four additional rounds of refinement and model building. The progress of the refinement of the lysozyme structure is illustrated in Fig. 2.

Water molecules were included after refinement round 5 when the R factor had dropped below 0.25. Water molecules were selected on the basis of: (*a*) well defined electron density, (*b*) that they should participate in reasonably good hydrogen bonding with either protein atoms or other water molecules and (*c*) that their electron density was higher than 1.5σ for the map.*

* Atomic coordinates and structure factors have been deposited with the Protein Data Bank, Brookhaven National Laboratory (Reference: 1LMN, R1LMNSF). Free copies may be obtained through The Managing Editor, International Union of Crystallography, 5 Abbey Square, Chester CH1 2HU, England (Reference: SE0151).

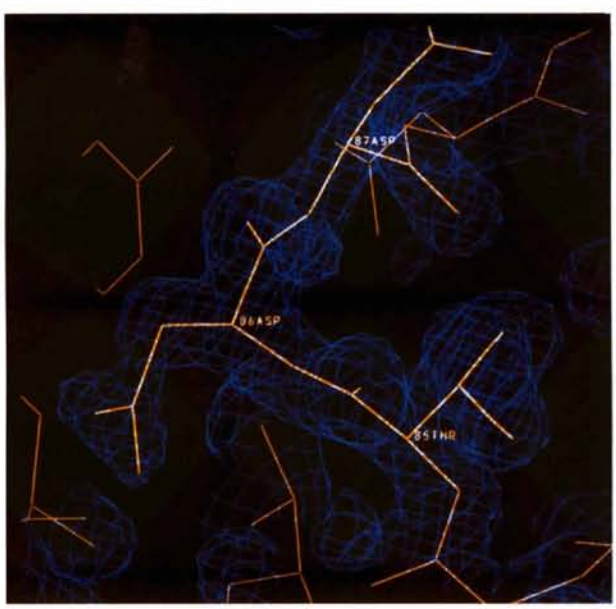

Fig. 4. Observed electron density contoured at 1.5σ (0.45 e Å^{-3}) in the final $2F_o - F_c$ map for an aspartic acid in position 86 of the lysozyme structure.

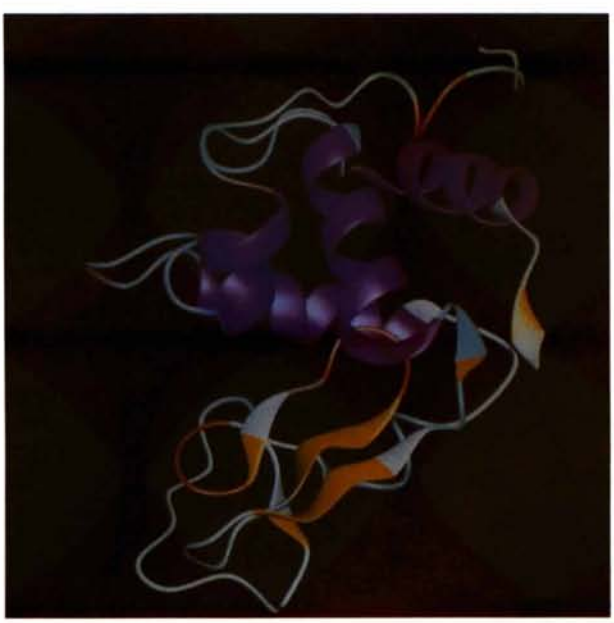

Fig. 5. A ribbon drawing of the rainbow trout lysozyme made by the program *QUANTA*. The α-helices are coloured violet, the β-strands are yellow, and the three-turn and four-turn are coloured orange and light blue, respectively.

Results

Interpretation of electron-density maps

After the first refinement round, all main-chain atoms were present in well defined electron density. The greatest adjustments were necessary at the C-terminal end, from residues 117 to 129. This region lies on the surface and is more flexible than inner parts of the molecule. Some rebuilding was also carried out at the N terminus, but only slight adjustments were necessary in the interior and more stable part of the enzyme. Residues 99–106, which form a loop on the surface of the enzyme, were clearly folded differently in RBTL than in the HEWL model. This is illustrated in Fig. 3.

The first electron-density map indicated that Asp4, Arg10, Gln82 and Asn117 in the initial model obviously were in wrong orientations. These sites are occupied by smaller amino acids in hen egg-white lysozyme. In order to avoid serious steric collisions in the RBTL, the larger side chains of these amino acids clearly had to point in other directions and have another orientation. Since it was difficult to find well defined electron density in the map, they were omitted from refinement and model building at this stage.

Apart from Lys73, Gln118, Asp119 and Arg121, where final electron density is still diffuse, all side chains in the structure have been located. Asp4, Asn113, Gln118 and Arg121 have side chains with χ_1 values which deviate from the mean χ_1 value by more than 2 standard deviations from ideality (Laskowski, MacArthur, Moss & Thornton, 1993). This is a general feature with the most poorly ordered residues lying on the surface of the molecule.

With the exception of these amino acids, all main- and side-chain atoms have well defined electron density. 127 ordered water molecules have been located around the RBTL molecule. Water molecules where B factors became greater than 80 Å^2 during the refinement, were omitted from the structure.

During the earliest stages of the structure determination, the complete gene sequence became available (Dautigny *et al.*, 1991). This was found to agree fully with the observed electron-density maps. The crystals used in the data collection were grown from a mixture of about 80% of type I and 20% of type II lysozyme. Electron-density maps show well defined density for an aspartic acid in position 86 (see Fig. 4). However, since Ala and Asp both have a C_β it is still possible that both forms are present in the crystal. If only Ala is present there would be no density for the carboxyl group.

The side chain of Asp86 is involved in a network of hydrogen bonds with an intramolecular interaction between OD2 of Asp86 and the main-chain amide group of the N-terminal Lys1 residue. This contact may have an important stabilizing effect on the N-terminus of the molecule. In addition, two intermolecular hydrogen bonds are formed between OD1 and OD2 of amino acid 86 and NE of Arg79 in a neighbouring molecule. OD2 also makes a hydrogen bond to water molecule 176. None of these interactions would be possible if an Ala was present in position 86, and it seems likely that the N-terminus would exhibit greater flexibility due to the missing hydrogen bond between the side chain of residue 86 and the main-chain amide group of Lys1.

Overall fold

Fig. 5 shows the overall fold of the enzyme in a ribbon drawing. Comparison of the overall fold of rainbow trout lysozyme with the chicken enzyme, shows that they are very similar. In common with HEWL and all the *c*-type lysozymes, RBTL consists of two domains separated by a deep cleft or crevice containing the active site. One domain, consisting of residues 40 to 84, contains some β-sheet structure, whereas the other containing the N- and C-terminal segments (residues 1–39 and 85–129), is more helical in nature. The packing of the rainbow trout lysozyme molecules in the trigonal cell (see Fig. 6) shows that the active-site cleft is not blocked by neighbouring molecules. Therefore, it should be possible to soak suitable substrates into the active-site cleft.

Secondary structure

The secondary structure of rainbow trout lysozyme comprises 40–45% α-helix. Helices are found mainly in the 'upper' domain (1–39, 85–129) whereas the 'lower' domain (40–84) is dominated by β-sheet structure and loop regions.

The secondary-structural elements are located in approximately the same sequential positions in rainbow trout lysozyme as in the chicken and human forms. The enzyme comprises four α-helices (labelled *A–D*) formed by residues 5–14, 25–36, 89–98 and 109–114. Short segments from residue 80–83 and 121–124 are defined as 3_{10} helices. Helices *A* and *C*, which lie on the protein surface partially exposed to solvent, surround a buried hydrophobic core which also includes helix *B*. The two domains of the molecule are linked by helix *C*. Residues

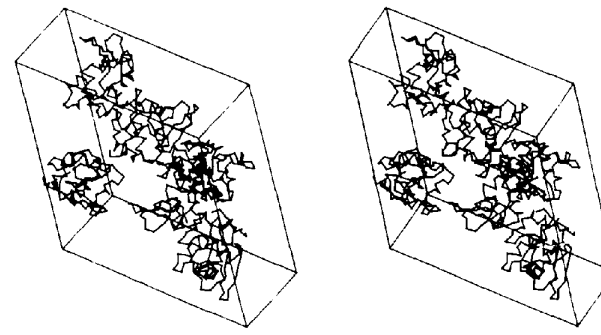

Fig. 6. Packing of rainbow trout lysozyme molecules in the trigonal unit cell.

41–79 form a smaller, mainly hydrophilic region containing a three-stranded (residues 43–45, 51–53, 58–59), antiparallel β-sheet (residues 42–60) connected to the hydrophobic core by a long coiled loop running from residue 61 to 78. This hydrophilic section consists of residues either on the outer surface of the molecule or lining the active-site cleft. The three-stranded β-sheet is a common element in *c*- and *g*-type lysozymes (Weaver *et al.*, 1985). Another small, two-stranded, β-sheet is formed by residues 1–2 and 39–40.

The polypeptide chain of rainbow trout lysozyme is extensively cross linked by a series of hydrogen bonds, and by four disulfide bridges. In common with all *c*-type lysozymes, the four disulfide bridges are formed between cysteines 6 and 127, 30 and 115, 64 and 80, and 76 and 94 (Blake *et al.*, 1965). The first two of these bonds link the N- and C-terminal segments in the first section of the molecule, whereas the third bridge is found in the hydrophilic part. The final disulfide bridge connects the two domains in the enzyme.

The amino-acid sequence

The amino-acid sequences of the rainbow trout, chicken and human lysozyme are compared in Fig. 7. Residues in the primary structure of HEWL, TEWL and HUML which differ from amino acids in RBTL are marked with boxes. Like all mammalian lysozymes, human lysozyme consists of 130 residues (Artymiuk & Blake, 1981). The extra amino acid is found in the hairpin loop between two β-strands (43–45 and 51–53) and is inserted between residues 47 and 48. As mentioned previously, the only difference in the primary structure of the two rainbow trout lysozymes is in position 86.

It can be seen from the figure that the amino-acid sequences are most conserved from residues 39 to 71 which form the β-sheet region. In view of this, it is not surprising that the three-stranded β-sheet is found to be conserved in all *c*- and *g*-type lysozymes (Weaver *et al.*, 1985). The primary structure is less well conserved in areas which form the α-helixes in the N- and C-terminal regions of the lysozyme molecules. Another important point is that the primary structure is more variable in the loops than in regions with more rigid secondary-structure elements. The rainbow trout lysozymes contain four more glycine residues (residues 19, 77, 106 and 128) in loop regions than HEWL. This will impart a greater degree of conformational flexibility to the fish enzymes – a factor which may explain their relatively high activity at temperatures as low as 277 K (Grinde *et al.*, 1988). The figure also emphasizes that the amino-acid sequences also show great variation in the C-terminal region.

Distribution of side chains

The majority of the non-polar side chains lie in the interior of the molecule, but are not distributed uniformly throughout the polypeptide chain. Apart from Ala42, no hydrophobic residues are present in the conserved β-sheet area (35–55) and, apart from Leu120, none lie

	1	2	3	4	5	6	7	8	9	10	11	12	13	14	15	16	17	18	19	20	21	22	23	24	25	26
HEWL	lys	val	phe	gly	arg	cys	glu	leu	ala	ala	ala	met	lys	arg	his	gly	leu	asp	asn	tyr	arg	gly	tyr	ser	leu	gly
TEWL	lys	val	tyr	gly	arg	cys	glu	leu	ala	ala	ala	met	lys	arg	leu	gly	leu	asp	asn	tyr	arg	gly	tyr	ser	leu	gly
HUML	lys	val	phe	glu	arg	cys	glu'	leu	ala	arg	thr	leu	lys	arg	leu	gly	met	asp	gly	tyr	arg	gly	ile	ser	leu	ala
RBTL I	lys	val	tyr	asp	arg	cys	glu	leu	ala	arg	ala	leu	lys	ala	ser	gly	met	asp	gly	tyr	ala	gly	asn	ser	leu	pro
RBTL II	lys	val	tyr	asp	arg	cys	glu	leu	ala	arg	ala	leu	lys	ala	ser	gly	met	asp	gly	tyr	ala	gly	asn	ser	leu	pro

	27	28	29	30	31	32	33	34	35	36	37	38	39	40	41	42	43	44	45	46	47	ω	48	49	50	51
HEWL	asn	trp	val	cys	ala	ala	lys	phe	glu	ser	asn	phe	asn	thr	gln	ala	thr	asn	arg	asn	thr	-	asp	gly	ser	thr
TEWL	asn	trp	val	cys	ala	ala	lys	phe	glu	ser	asn	phe	asn	thr	his	ala	thr	asn	arg	asn	thr	-	asp	gly	ser	thr
HUML	asn	trp	met	cys	leu	ala	lys	trp	glu	ser	gly	tyr	asn	thr	arg	ala	thr	asn	tyr	asn	ala	gly	asp	arg	ser	thr
RBTL I	asn	trp	val	cys	leu	ser	lys	trp	glu	ser	ser	tyr	asn	thr	gln	ala	thr	asn	arg	asn	thr	-	asp	gly	ser	thr
RBTL II	asn	trp	val	cys	leu	ser	lys	trp	glu	ser	ser	tyr	asn	thr	gln	ala	thr	asn	arg	asn	thr	-	asp	gly	ser	thr

	52	53	54	55	56	57	58	59	60	61	62	63	64	65	66	67	68	69	70	71	72	73	74	75	76	77
HEWL	asp	tyr	gly	ile	leu	gln	ile	asn	ser	arg	trp	trp	cys	asn	asp	gly	arg	thr	pro	gly	ser	arg	asn	leu	cys	asn
TEWL	asp	tyr	gly	ile	leu	gln	ile	asn	ser	arg	trp	trp	cys	asn	asp	gly	arg	thr	pro	gly	ser	lys	asn	leu	cys	asn
HUML	asp	tyr	gly	ile	phe	gln	ile	asn	ser	arg	tyr	trp	cys	asn	asp	gly	lys	thr	pro	gly	ala	lys	asn	ala	cys	his
RBTL I	asp	tyr	gly	ile	phe	gln	ile	asn	ser	arg	tyr	trp	cys	asp	asp	gly	arg	thr	pro	gly	ala	lys	asn	val	cys	gly
RBTL II	asp	tyr	gly	ile	phe	gln	ile	asn	ser	arg	tyr	trp	cys	asp	asp	gly	arg	thr	pro	gly	ala	lys	asn	val	cys	gly

	78	79	80	81	82	83	84	85	86	87	88	89	90	91	92	93	94	95	96	97	98	99	100	101	102	103
HEWL	ile	pro	cys	ser	ala	leu	leu	ser	ser	asp	ile	thr	ala	ser	val	asn	cys	ala	lys	lys	ile	val	ser	asp	gly	asn
TEWL	ile	pro	cys	ser	ala	leu	leu	ser	ser	asp	ile	thr	ala	ser	val	asn	cys	ala	lys	lys	ile	ala	ser	gly	gly	asn
HUML	leu	ser	cys	ser	ala	leu	leu	gln	asp	asp	ile	ala	pro	ala	val	ala	cys	ala	lys	arg	val	val	arg	asp	pro	gln
RBTL I	ile	arg	cys	ser	gln	leu	leu	thr	asp	asp	asn	thr	val	ala	ile	arg	cys	ala	lys	arg	val	val	leu	asp	pro	asp
RBTL II	ile	arg	cys	ser	gln	leu	leu	thr	*ala*	asp	asn	thr	val	ala	ile	arg	cys	ala	lys	arg	val	val	leu	asp	pro	asp

	104	105	106	107	108	109	110	111	112	113	114	115	116	117	118	119	120	121	122	123	124	125	126	127	128	129
HEWL	gly	met	asn	ala	trp	val	ala	trp	arg	asn	arg	cys	lys	gly	thr	asp	val	gln	ala	trp	ile	arg	gly	cys	arg	leu
TEWL	gly	met	asn	ala	trp	val	ala	trp	arg	asn	arg	cys	lys	gly	thr	asp	val	his	ala	trp	ile	arg	gly	cys	arg	leu
HUML	gly	ile	arg	ala	trp	val	ala	trp	arg	asn	arg	cys	gln	asn	arg	asp	val	arg	gln	tyr	val	gln	gly	cys	gly	val
RBTL I	gly	ile	gly	ala	trp	val	ala	trp	arg	asn	his	cys	gln	asn	gln	asp	leu	arg	ser	tyr	val	ala	gly	cys	gly	val
RBTL II	gly	ile	gly	ala	trp	val	ala	trp	arg	asn	his	cys	gln	asn	gln	asp	leu	arg	ser	tyr	val	ala	gly	cys	gly	val

Fig. 7. Comparison of the amino-acid sequences from rainbow trout lysozyme type I and II with those from HEWL (hen egg-white lysozyme), TEWL (turkey egg-white lysozyme) and HUML (human lysozyme). Residues in HEWL, TEWL and HUML which differ from amino acids in the rainbow trout lysozymes, are marked with boxes. The extra amino acid in HUML inserted between residue 47 and 48, is represented in the table by an ω. The only difference between the RBTL type I and II is found in position 86 where Ala86 in the type II form is written in italics.

between residues 111 and 124. Except for Asp101 and Asp103, a completely hydrophobic region is also found from residues 98 to 111. The deep active-site cleft thus seems to be divided into two regions with markedly different character. The 'upper' helical domain has a considerable proportion of non-polar side chains, which form a striking hydrophobic core built up of tryptophans 28, 108 and 111 and isoleucine 105, and is probably a source of great structural stability. The 'lower', smaller, domain has relatively few hydrophobic groups and contains the important hydrogen-bonded network in the β-sheet region which is also found in other *c*-type lysozymes (Phillips, 1967; Artymiuk & Blake, 1981).

There are a number of hydrophobic groups on the surface of the molecule, for example, Val2, Trp34, Val75, Val90 and Leu100. Several such residues including Phe56, Ile58, Trp63, Val98, Trp108 and Val109 also form part of the surface of the active-site cleft.

The active site

Comparison of the active-site cleft of rainbow trout lysozyme with that in the chicken enzyme, shows that they are almost identical. Residues lining the cleft, which can accommodate six oligosaccharide units in sites which are usually termed *A* to *F* (Blake *et al.*, 1967), include the β-sheet in the lower domain (residues 43, 44, 46, 52, 56–59), the carboxy terminus of the second α-helix (residues 34–36), the loop connecting the third and fourth helix (residues 98 and 101–103), the amino terminus of the last helix (residues 107–110 and 112), and residues 62, 63 and 73. Within the limits of accuracy of the structure determinations, the catalytically active residues Glu35 at the end of the second helix and Asp52 in the second β-strand, have similar positions and orientations in RBTL and HEWL. This suggests that the rainbow trout enzyme has the same catalytic mechanism as that proposed for chicken lysozyme. The roles of the catalytically active residues Asp52 and Glu35 of chicken lysozyme have been investigated by site-directed mutagenesis where each residue was replaced by its corresponding amide (Malcolm *et al.*, 1989). The D52N mutant exhibits approximately 5% of the wild-type lytic activity against *M. luteus* cell walls, while there is no measurable activity associated with the E35Q mutant.

The catalytic residue Glu35 is involved only in a single hydrogen bond, from side-chain atom OD2 to a water molecule (Wat201). Since our crystals of RBTL were grown at pH 9.5–10.5, this glutamic acid will probably be in the unionized form and cannot be a proton donor. The environment of this residue is seen in Fig. 8. The side chain of Glu35 is buried in a relatively hydrophobic pocket formed by the side chains of Gln57 (the methylene C atoms C_β, C_γ), Trp108, Val109 and Ala110, making the pK_a abnormally high ($pK_a = 6.5$, Imoto, Johnson, North, Phillips & Rupley, 1972) compared with that of the normal glutamic acid residue ($pK_a = 4.4$, Roxby & Tanford, 1971). The hydrophobic residue, Trp108, which is conserved in all *c*-type lysozymes known so far (Nitta & Sugai, 1989), has been shown, together with an electrostatic interaction from Asp52, to play an important role in keeping the pK_a of Glu35 abnormally high (Inoue *et al.*, 1992). The high pK_a of Glu35 is considered to be critical for this residue in order to serve as general acid catalyst in the glycosidase activity of lysozyme at higher pH's. The positive pole of the short helix from Val109 to His114 points almost directly towards the carboxy group of Glu35, thereby helping to stabilize the negative charge that develops on this group during the general acid catalysis (Blake *et al*, 1967). Amino acids in the cluster of hydrophobic residues (28, 105 and 108) and the short helix are highly conserved in all *c*-type lysozymes (Jolles & Jolles, 1984). Furthermore, amino acids which are found to play an important role in the binding of substrates to the active-site cleft in HEWL (Strynadka & James, 1991), including Asn46, Asn59, Trp63, Asp101, Ala107, Trp108 and Val109, are also conserved in the rainbow trout lysozyme.

Asp52, the second amino acid which is believed to play an important role in the hydrolysis of oligosaccharides, is part of the three-stranded antiparallel β-sheet and has a side chain which protrudes into the active-site cleft in a more hydrophilic environment than Glu35 (see Fig. 9). As a consequence, the pK_a value of this residue is lower than for Glu35 and it is in an ionized form during catalysis. The carbonyl group is thus believed to stabilize the oxocarbonium intermediate which develops during the general acid catalysis by electrostatic interaction (Blake *et al.*, 1967). The recently solved structure of a modified human lysozyme, in which the catalytic Asp residue was replaced by Glu, has shown that the low catalytic activity of this mutant is due to a positional and orientational change in the Glu carboxyl group (Harata, Muraki, Hayashi & Jigami, 1992) implying that this residue contributes with more than simply an electrostatic stabilization of the intermediate in the catalysis reaction.

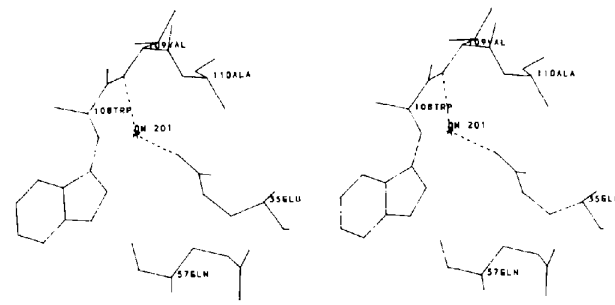

Fig. 8. The environment of the catalytic residue. Hydrogen bonds are shown as thin, broken lines. Only side chains critical to the present discussion are shown.

The solvent-exposed OD2 in Asp52 in RBTL forms three hydrogen bonds to water molecules (142, 202 and 245). Wat142 makes a bridge to OE1 in Gln57, and Wat202 is hydrogen bonded to Wat201 which then bridges across to the main-chain amide group of Val 109 (see Fig 9). Wat201 also forms a hydrogen bond to the carboxyl group in the side chain of Glu35. Thus, the catalytically active amino acids are hydrogen bonded to each other through an extensive water-mediated network of hydrogen bonds. This indicates that several water molecules are closely associated with the two residues that can attack the positively charged oxocarbonium ion which is believed to develop during the hydrolysis.

The second O atom in this carboxylate group (Asp52), OD1, is involved in a hydrogen-bonded network with the side chains of Asn46, Asp48, Ser50 and Asn59 (see Fig. 9). All these side chains are on the same side of the β-sheet as the side chain of Asp52.

The temperature factors

Fig. 10 shows the variation of the average main-chain and side-chain atomic temperature factors along the polypeptide chain. The mean B factor for protein atoms is 24.4 Å^2, and 44.2 Å^2 for solvent atoms. The average B factor for main-chain and side-chain atoms is 22.0 and 26.9 Å^2, respectively. The highest temperature factor for an accepted water molecule is 72.8 Å^2. The relative low average temperature factor for water is appropriate for water molecules belonging to the first water layer.

The B-factor plot shows that average B factors for the backbone atoms are highest for residues in the external loop regions. This is most clearly seen for residues 46–50 which form the β-bend between the 43–45 and 51–53 β-strands, and in the 61–80 loop region in the lower domain. These two loop regions contribute to the edges of the active-site cleft, and have greater mobility in order to accommodate an incoming substrate. The C-terminal region, particularly from residues 117 to 119, shows higher mobility than the N-terminus. The B-factor plot also emphasizes that the residues with side chains which have highest mean B factors, are mostly lysines, arginines, asparagines and aspartic acids.

Table 2. *Summary of refinement*

Resolution range (Å)	8.0–1.80
$R(=\sum \|F_o\| - \|F_c\| / \sum \|F_o\|)$	0.174
No. of reflections ($\|F\| > 3\sigma_F$)	16080
No. of protein atoms	999
No. of solvent atoms	127
R.m.s. deviations from ideal values	
Bond distances (Å)	0.013
Angle distances (Å)	0.044
Planar 1–4 distances (Å)	0.047
Planar groups (Å)	0.013
Chiral centers (Å^3)	0.038
Non-bonded contacts	
Single torsions (Å)	0.172
Multiple torsions (Å)	0.254
Hydrogen bonds (Å)	0.224

Reliability of the final model

Final refinement statistics are given in Table 2. The r.m.s. deviations from ideal values for bond lengths and angle distances of rainbow trout lysozyme are 0.013 and 0.044 Å, respectively. These values are in the normal range for protein structures of this size and at this resolution.

The Luzzati plot (Luzzati, 1952) given in Fig. 11, shows that the mean positional error for atoms in rainbow trout lysozyme is approximately 0.2 Å, but the curve rises after 0.25 in $\sin\theta/\lambda$. Table 3 which gives a survey over the completeness and the quality of the image-plate data, indicates that the lysozyme crystal diffracts well to 1.8 Å resolution. From 1.9 to 1.8 Å resolution 94 and 44% of the intensities are greater than $3\sigma_F$ and $5\sigma_F$, respectively.

The Ramachandran plot (Ramachandran & Ramakrishnan, 1968) seen in Fig. 12 shows the distribution of the torsion angles in the rainbow trout lysozyme structure. The majority of the main-chain dihedral angles determined by the program *PROCHECK* (Laskowski,

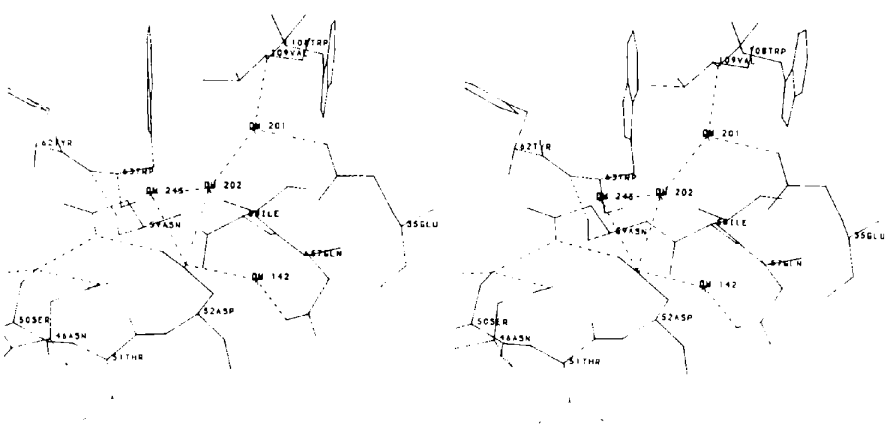

Fig. 9. The environment of the catalytic residue Asp52. Hydrogen bonds are seen as thin, broken lines. To ensure clarity, only those side chains that are in the region of Asp52 have been included.

Table 3. *Summary of completeness and quality of the image-plate data*

Resolution (Å)	No. of reflections	Completeness (%)	Fraction of reflections with $\|F\| > 1\sigma_F$	Fraction of reflections with $\|F\| > 3\sigma_F$	Fraction of reflections with $\|F\| > 5\sigma_F$
8.00–3.51	2317	95.7	1.00	1.00	0.99
3.51–2.83	2221	95.8	1.00	0.99	0.96
2.83–2.48	2197	95.3	1.00	0.98	0.94
2.48–2.26	2179	94.5	1.00	0.97	0.90
2.26–2.10	2171	93.6	1.00	0.96	0.84
2.10–1.98	2166	90.6	1.00	0.91	0.73
1.98–1.88	2148	87.3	1.00	0.87	0.60
1.88–1.80	2148	79.7	1.00	0.80	0.44
8.00–1.80	16080	91.6	1.00	0.94	0.81

MacArthur, Moss & Thornton, 1993) fall within acceptable areas and most of the remainder represent glycine residues. 92.9% of the residues in the structure are found in the most energetically favoured regions, and 7.1% are in additional allowed regions.

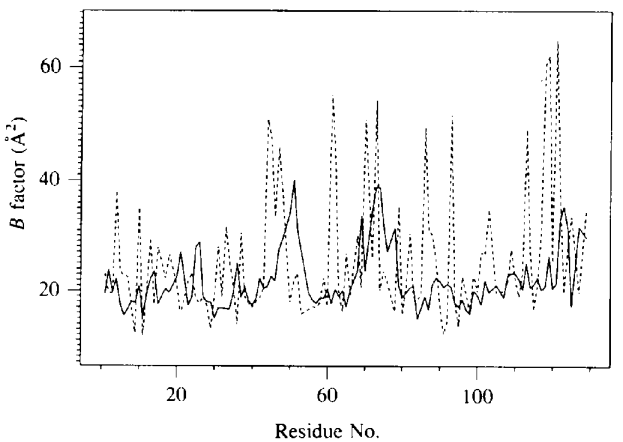

Fig. 10. Variation in isotropically refined temperature factors [B (Å^2)] along the polypeptide chain, averaged over main-chain and side-chain atoms. Full-drawn lines are seen between the average of values for main-chain atoms, while broken lines are drawn between the corresponding values for side chains.

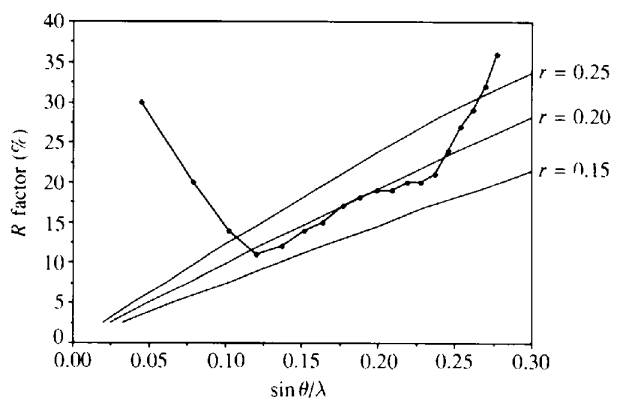

Fig. 11. Plot of R factor as a function of resolution. The straight lines show the theoretical dependence of the R factor on resolution for the coordinate errors shown on the right (Luzzati, 1952).

Discussion

Comparison with other c-type lysozymes

The three-dimensional structure of rainbow trout lysozyme is similar to previously solved structures of *c*-type lysozymes. The secondary-structure elements, α-helices and β-sheet, are found approximately in the same sequential positions in all the enzymes. Alignment of the rainbow trout, chicken, turkey and human lysozyme emphasizes that differences in secondary structures are found in loop areas, particularly on the surface of the enzymes. The region where the structures of RBTL and HEWL clearly show different folding is in the residues 101–106 external loop which forms part of the edge of the active-site cleft. Comparison of the structure of rainbow trout with the hen and turkey enzyme also emphasizes differences from amino acids 64 to 77 in a long exposed coiled-loop region in the lower β-sheet domain. All the lysozymes, but particularly the human

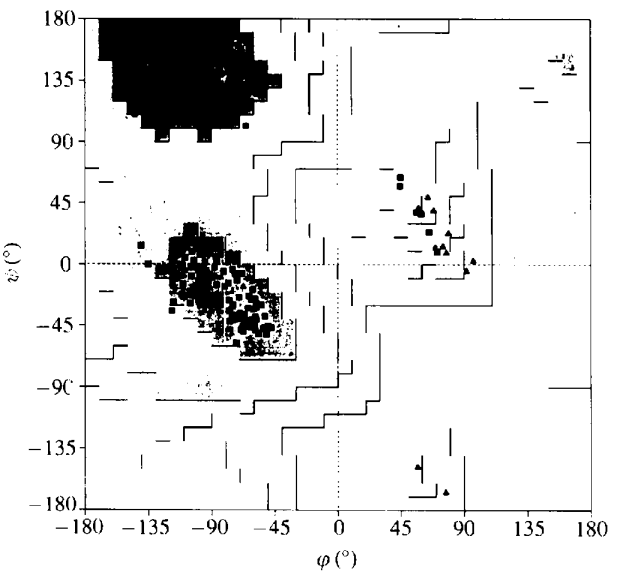

Fig. 12. The Ramachandran plot (Ramachandran & Sasisekharan, 1968) of the main-chain torsion angles (φ and ψ) for the final refined model of RBTL. Glycine residues are shown as triangles and all other residues as squares. The plot was produced with the program *PROCHECK* (Laskowski *et al.*, 1993).

form, have a different fold to RBTL in the 44–48 hairpin loop in the β-sheet. Differences, probably due to high flexibility, can also be seen between the chicken and rainbow trout enzyme in the loop connecting the first and second α-helix, and in the C-terminal end of the molecule.

R.m.s. differences in the main chain between RBTL and HEWL, HUML and TEWL are 0.75, 0.49 and 0.88 Å, respectively. The corresponding values for the side chains are 1.32, 1.25 and 1.37 Å. This indicates that the human enzyme is most homologous to the rainbow trout lysozyme both in three-dimensional structure and primary sequence.

From the present results, there is some reason to believe that the key to understanding why the rainbow trout lysozymes and specially the type I variant show high specific activity against a variety of bacteria which are not attacked by other lysozymes, is probably to be found in the loop areas of the enzymes. Differences in flexibility and loop folding will modulate substrate accessbility and thus the catalytic activity of the lysozymes. Another point is that differences in mobility and hydrophobicity in exterior loop regions on the surface of the enzymes could change their ability to penetrate into the cell wall of the bacteria.

The effect of temperature on activity for the rainbow trout lysozymes and HEWL was investigated at pH 6.2 over the temperature range 277–345 K (Grinde *et al.*, 1988). The resulting data indicated that the fish enzymes have higher catalytic activity below 293 K than the hen enzyme. This is probably an evolutionary adaptation in arctic fish species. The rainbow trout lysozymes contain, as mentioned earlier, four more glycine residues (residues 19, 77, 106 and 128) in loops than the HEWL molecule. It is not unlikely that these extra glycines give increased flexibility to the loop regions, a factor which may explain their high activity at low temperatures.

Comparison with g-type lysozymes

g-Type lysozymes differ from *c*-type lysozymes in molecular weight, amino-acid composition and immunological properties (Arnheim, Hindenburg, Begg & Morgan, 1973). There is no overall sequence homology between the two families of lysozymes, but limited sequence correspondence occurs, for example, in the active sites and other limited segments (Weaver *et al.*, 1985). Two crystal structures of *g*-type lysozymes, from Embden goose and Australian black swan, have been determined (Grütter, Weaver & Matthews, 1983; Isaacs, Machin & Masakuni, 1985). The black swan goose-type egg-white lysozyme (SELg) consists of 185 amino-acid residues ($M_r = 20400$) and its amino-acid sequence (Simpson, Begg, Dorow & Morgan, 1980) closely resembles the Embden goose egg-white lysozyme (GEWL), differing in only six of the residues (Simpson & Morgan, 1983). Coordinates of the SELg were kindly provided by Professor N. W. Isaacs, University of Glasgow, in order to compare this structure with the structure of *c*-type lysozyme from rainbow trout.

In common with Embden goose lysozyme, the structure of SELg consists predominantly of seven α-helices (residues 18–24, 30–46, 49–59, 63–74, 110–130, 136–149 and 169–180) and three small irregular strands of antiparallel β-sheet structure (residues 84–86, 89–91 and 95–97). As for the *c*-type lysozymes, the *g*-type enzyme is divided into two domains separated by a deep cleft which contains the acidic residues (Glu73 and Asp86). These residues, located on either side of the cleft with a distance of 10 Å between the carboxyl groups, could be equivalent to the catalytically active Glu35 and Asp52 of HEWL (Schoentgen, Jolles & Jolles, 1982). Fig. 13 shows a comparison of the C_α diagonal plot of SELg (upper left) and RBTL (lower right). The C_α plot of the *c*-type lysozyme is aligned with the plot of the *g*-type enzyme to give the best structural correspondence between the enzymes. The figure indicates that the region with most structural similarity is found in the β-sheet area from residues 50 to 65 in RBTL and 90 to 105 in SELg. Spatial correspondence is also seen from residues 20 to 40 and 60 to 80 which comprise the second α-helix in the *c*-type lysozyme and the fourth helix in the *g*-type enzyme, respectively, and in the loop regions.

Previous comparisons of the three-dimensional structure of GEWL with both HEWL and bacteriophage T4 lysozyme (T4L) have shown that apart from residues 1–46 in the amino-terminal region, essentially every residue of GEWL has a counterpart either in the hen lysozyme or in the phage lysozyme or both (Grütter *et al.*, 1983). This structural correspondence strongly suggests that all three lysozymes have evolved from a common precursor. Parts

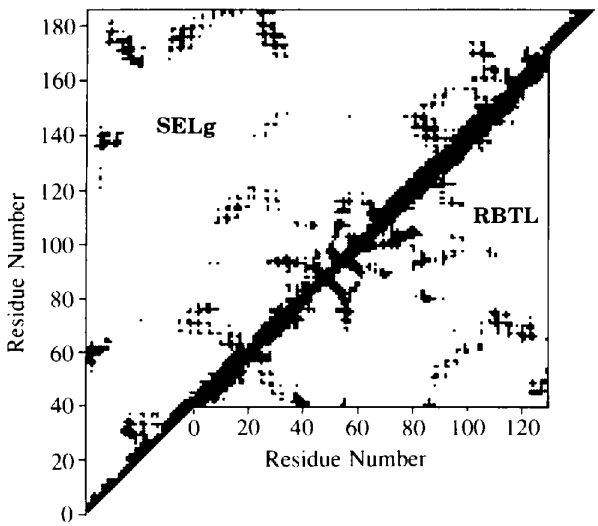

Fig. 13. Comparison of the C_α diagonal plot of the *g*-type lysozyme from the egg white of the Australian black swan on the upper left and the *c*-type lysozyme from the rainbow trout on the lower right. The plots are aligned to emphasize structural similarities.

of four α-helices, together with the three-stranded β-sheet, occur in all three lysozymes, and presumably include the catalytically essential element of the respective structures. These common residues constitute the core of the molecule and form both sides of the active-site cleft.

Comparisons of the lysozymes from rainbow trout and black swan show that the first three α-helices of RBTL correspond approximately to the third, fourth and the N-terminal end of the fifth helix of SELg. The N-terminal segment, residues 1–17, in RBTL and other *c*-type lysozymes, has a counterpart in SELg from residues 41 to 57 which comprise the C-terminal end of the second helix and the entire third helix. The r.m.s. value for the backbone between the enzymes in this area is 3.1 Å so that the correspondence is not particularly good. The alignment of the second helix of RBTL (residues 23–39) with the fourth helix in SELg (residues 61–77) gives an r.m.s. value of 0.6 Å. The C termini of these helices form part of the active-site clefts and contain the catalytically active glutamic acids (Glu35 and Glu73 in RBTL and SELg, respectively). It is, therefore, not surprising that this part of the enzyme is structurally conserved. Alignment of residues 51–64 in RBTL and 89–102 in SELg, which are part of the structurally conserved β-sheet region and form part of the lining of the active-site cleft, also give a low r.m.s. value of 1.0 Å.

The long flexible coiled loop region from residue 65 to 81 does not have a counterpart in the black swan lysozyme. The structural correspondence between the loop (residues 83–87) before the third helix in RBTL and the loop in connection with the fifth helix (105–109) in SELg is also fairly poor (r.m.s. = 1.9 Å). Alignment of the third helix (residues 90–103) in the *c*-type lysozyme with the amino-terminal end of helix five in the *g*-type enzyme gives an r.m.s. value of 1.7 Å. The corresponding value for the structural similarity between the N-terminal part of the fourth helix and the carboxy terminal of helix six in the same enzymes is 1.4 Å. Residues 110–118 in RBTL, which comprise the C terminus of the fourth α-helix and a loop in elongation to it, gives an r.m.s. deviation of 1.7 Å when fitted to the N terminus of the seventh helix in SELg. The last structural correspondence is found in the C-terminal part of the rainbow trout molecule (residues 120–127) which comprises a 3_{10} helix and a loop region and the C terminus of the last α-helix of the swan enzyme (residues 177–184), giving an r.m.s. deviation of 2.0 Å. Alignment of the two regions in the enzymes with the closest similarity in three-dimensional structure (residues 23–39 and 51–64 in RBTL, and residues 61–77 and 89–102 in SELg) gives an r.m.s. value of 1.1 Å. Fig. 14 illustrates a superimposition of the *c*- and *g*-type lysozymes where these two areas (coloured red) in the enzymes are aligned. The figure emphasizes again that the three-dimensional structures are most conserved around the active-site cleft. The r.m.s. deviations between the RBTL and SELg were generated using the program *QUANTA* which has been developed by Molecular Simulations, Inc.

Comparison of the rainbow trout lysozyme and the black swan egg-white enzyme thus shows that structural similarities are predominantly found in regions with α-helices and particularly β-sheet structure. The first helix and the N-terminal part of the second α-helix in SELg and the two loop regions between the fifth and sixth helix (residues 125–142) and between the last two helices (residues 149–167) in the swan enzyme have no counterpart in RBTL.

Differences between the type I *and* II *forms of RBTL*

Electron-density maps for the RBTL structure showed that it was impossible to distinguish the two lysozyme forms if both were present in the crystals. As previously mentioned, the type II variant of the enzyme has an alanine in this position (Dautigny *et al.*, 1991), and is shown to be much more potent against a variety of pathogenic bacteria than the type I form (Grinde, 1989*a*). It seems unlikely that a single amino-acid change in a loop region on the surface of a enzyme will alter the secondary or three-dimensional structure of the enzyme to an extent which can explain the differences in activity.

Residue 86 is part of a short loop in elongation of the 3_{10} helix (residues 80–84), and has a side chain which extends into the solvent not far from the N-terminus. The distance between C_α atoms of Asp86 and Lys1 is 5.0 Å. Residue 86 is neither part of, or in close connection with,

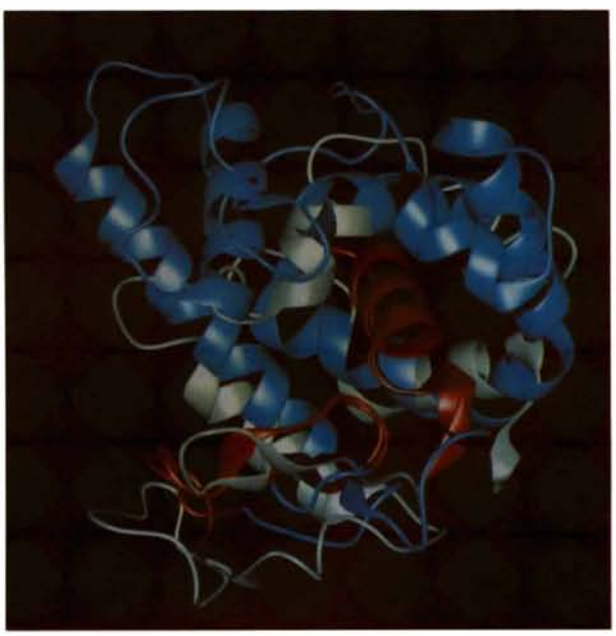

Fig. 14. A superimposition of RBTL (grey) and SELg (blue) in a cartoon drawing. The two most conserved regions in the enzymes (residues 23–39 and 51–64 in RBTL, and 61–77 and 89–102 in SELg) are aligned and coloured red in the picture.

the active-site cleft. It is, therefore, unlikely that differences in antibacterial specificity are related to structural or electrostatic changes in the active site of the two type of enzymes. It seems more likely that differences in the hydrophobicity of a part of the lysozyme surfaces affect their ability to recognise and attack bacterial cell walls.

Studies of mutant lysozymes of bacteriophage T4 suggest that the C-terminal domain participates in the binding and orientation of the peptide which cross links adjacent oligosaccharide strands within the cell wall of *Escherichia coli* (Grütter & Matthews, 1982). The peptide must extend across the face of the upper C-terminal lobe of the lysozyme molecule (Anderson, Grütter, Remington, Weaver & Matthews, 1981), and pass the immediate vicinity of Arg125 and Glu128 which are involved in binding and alignment of the peptide. These interactions may help to position the saccharide part of the cell wall for optimal hydrolysis in the active-site cleft. Hen egg-white lysozyme has no counterpart for this C-terminal lobe region, and has broader specificity but lower efficiency than the T4 phage lysozyme. It is not impossible that residue 86 in rainbow trout lysozyme has a similar function as Arg125 and Glu128 in the T4 molecule in the binding of the saccharide unit of the cell wall to the enzyme.

The more active type II RBTL has a small and hydrophobic alanine residue in position 86, rather than the hydrophilic and larger Asp in type I. It is not likely that this difference in the size of the side chains would alter the conformation of the exterior loop region. It seems more reasonable that, due to electrostatic repulsion, the charged side chain of aspartic acid may experience greater difficulty in penetrating the cell wall than does the neutral and smaller alanine residue. This may well influence the specificity of the different lysozymes since the composition and charge of cell walls differs from bacterium to bacterium. Position 86 is occupied by a serine in HEWL so that its specificity will be different to RBTL. Like the RBTL type I variant, the human lysozyme has an Asp in this strategic position and may have a similar bacterial specificity.

Kinetic experiments using the non-charged oligomer chitin, which has a well defined chemical structure and properties, as substrate showed that there was no significant difference in enzymatic activity between the rainbow trout lysozymes and the chicken enzyme (Grinde, Jolles & Jolles, 1988). Earlier studies have suggested that there are considerable differences in the activity of lysozymes against small substrates and their activity against bacterial cell walls (Imoto *et al.*, 1972). These results confirm that the reason for differences in catalytic activity are found in the complex nature of bacterial cell walls rather than in the nature of the oligomeric substrates.

The present study has shown that rainbow trout lysozyme is a typical *c*-type lysozyme and suggest that its high activity at low temperature is a consequence of greater flexibility in the loop regions. Differences in the antibiotic activity of the two forms of RBTL are probably due to small differences in the hydrophobicity of a small surface region. Crystallographic studies of complexes between RBTL and a number of oligosaccharides are under way.

This work has been supported by the Norwegian Research Council for Science and the Humanities (NAVF), and we thank Professor N. W. Isaacs, University of Glasgow, for supplying us with the atomic coordinates of the Australian black swan lysozyme.

References

ANDERSON, W. F., GRÜTTER, M. G., REMINGTON, S. J., WEAVER, L. H. & MATTHEWS, B. W. (1981). *J. Mol. Biol.* **147**, 523–543.

ARNHEIM, N., HINDENBURG, A., BEGG, G. S. & MORGAN, F. J. (1973). *J. Biol. Chem.* **248**, 8036–8042.

ARTYMIUK, P. J. & BLAKE, C. C. F. (1981). *J. Mol. Biol.* **152**, 737–762.

BLAKE, C. C. F., JOHNSON, L. N., MAIR, G. A., NORTH, A. C. T., PHILLIPS, D. C. & SARMA, V. R. (1967). *Proc. R. Soc. London Ser. B*, **167**, 378–388.

BLAKE, C. C. F., KOENIG, D. F., MAIR, G. A., NORTH, A. C. T., PHILLIPS, D. C. & SARMA, V. R. (1965). *Nature (London)*, **206**, 757–761.

BROOKS, B. R., BRUCCOLERI, R. E., OLAFSON, B. D., STATES, D. J., SWAMINATHAN, S. & KARPLUS, M. (1983). *J. Comp. Chem.* **4**, 187–217.

COLLABORATIVE COMPUTATIONAL PROJECT, NUMBER 4 (1994). *Acta Cryst.* D**51**, 760–763.

CROWTHER, R. A. (1972). *The Molecular Replacement Method*, edited by M. G. ROSSMANN, pp. 173–178. New York: Gordon & Breach.

CROWTHER, R. A. & BLOW, D. M. (1967). *Acta Cryst.* **23**, 544–548.

DAUTIGNY, A., PRAGER, E. M., PHAM-DINH, D., JOLLES, J., PAKDEL, F., GRINDE, B. & JOLLES, P. (1991). *J. Mol. Evol.* **32**, 187–198.

FITZGERALD, P. M. D. (1988). *J. Appl. Cryst.* **21**, 273–278.

GRINDE, B. (1989*a*). *J. Fish Dis.* **12**, 95–104.

GRINDE, B. (1989*b*). *FEMS Microbiol. Lett.* **60**, 179–182.

GRINDE, B., JOLLES, J. & JOLLES, P. (1988). *Eur. J. Biochem.* **173**, 269–273.

GRINDE, B., LIE, Ø., POPPE, T. & SALTE, R. (1988). *Aquaculture*, **68**, 299–304.

GRÜTTER, M. G. & MATTHEWS, B. W. (1982). *J. Mol. Biol.* **154**, 525–535.

GRÜTTER, M. G., WEAVER, L. H. & MATTHEWS, B. W. (1983). *Nature (London)*, **303**, 828–831.

HARATA, K., MURAKI, M., HAYASHI, Y. & JIGAMI, Y. (1992). *Protein Sci.* **1**, 1447–1453.

HENDRICKSON, W. A. (1985). *Methods Enzymol.* **115**, 252–270.

HODSON, J. M., BROWN, G. M., SIEKER, L. C. & JENSEN, L. H. (1990). *Acta Cryst.* B**46**, 54–62.

IMOTO, T., JOHNSON, L. N., NORTH, A. C. T., PHILLIPS, D. C. & RUPLEY, J. A. (1972). *The Enzymes*, 3rd ed., Vol. 7, edited by P. BOYER, pp. 665–868. New York: Academic Press.

INOUE, M., YAMADA, H., YASUKOCHI, T., KUROKI, R., MIKI, T., HORIUCHI, T. & IMOTO, T. (1992). *Biochemistry*, **31**, 5545–5553.

ISAACS, N. W., MACHIN, K. J. & MASAKUNI, M. (1985). *J. Biol. Sci.* **38**, 13–22.

JOLLES, P. & JOLLES, J. (1984). *Mol. Cell. Biochem.* **63**, 165–189.

JONES, T. A. (1985). *Methods Enzymol.* **115**, 157–170.

LASKOWSKI, R. A., MACARTHUR, M. W., MOSS, D. S. & THORNTON, J. M. (1993). *J. Appl. Cryst.* **26**, 283–291.

LATTMAN, E. E., NOCKOLDS, C. E., KRETSINGER, R. H. & LOVE, W. E. (1971). *J. Mol. Biol.* **60**, 271–277.

LUZZATI, P. V. (1952). *Acta Cryst.* **5**, 802–810.
MALCOLM, B. A., ROSENBERG, S., COREY, M. J., ALLEN, J. S., BAETSELIER, A. D. & KIRSCH, J. F. (1989). *Proc. Natl Acad. Sci. USA*, **86**, 133–137.
NITTA, K. & SUGAI, S. (1989). *Eur. J. Biochem.* **182**, 111–118.
PEPYS, M. B., HAWKINS, P. N., BOOTH, D. R., VIGUSHIN, D. M., TENNENT, G. A., SOUTAR, A. K., TOTTY, N., NGUYEN, O., BLAKE, C. C. F., TERRY, C. J., FEEST, T. G., ZALIN, A. M. & HSUAN, J. J. (1993). *Nature (London)*, **362**, 553–557.
PHILLIPS, D. C. (1967). *Proc. Natl Acad. Sci. USA*, **57**, 484–495.
RAMACHANDRAN, G. N. & RAMAKRISHNAN, C. (1968). *Adv. Protein. Chem.* **23**, 283–437.
ROXBY, R. & TANFORD, C. (1971). *Biochemistry*, **10**, 3348–3352.
SALTON, M. R. J. & GHUYSEN, J. M. (1959). *Biochim. Biophys. Acta*, **36**, 552–554.
SALTON, M. R. J. & GHUYSEN, J. M. (1960). *Biochim. Biophys. Acta*, **45**, 355–363.
SCHOENTGEN, F., JOLLES, J. & JOLLES, P. (1982). *Eur. J. Biochem.* **123**, 489–497.
SIMPSON, R. J., BEGG, G. S., DOROW, D. S. & MORGAN, F. J. (1980). *Biochemistry*, **19**, 1814–1819.
SIMPSON, R. J. & MORGAN, F. J. (1983). *Biochim. Biophys. Acta*, **744**, 349–351.
STRYNADKA, N. C. J. & JAMES, M. N. G. (1991). *J. Mol. Biol.* **220**, 401–424.
WEAVER, L. H., GRUTTER, M. G., REMINGTON, S. J., GRAY, T. M., ISAACS, N. W. & MATTHEWS, B. W. (1985). *J. Mol. Evol.* **21**, 97–111.